Interaction Characteristics with Bovine Serum Albumin and Retarded Nitric Oxide Release of $ZCVI_4$-2, a New Nitric Oxide-Releasing Derivative of Oleanolic Acid

Jianjun Zhang,[a] Yuan Gao,*[,b] Feng Su,*[,a] Zhenhua Gong,[a] and Yihua Zhang[c]

[a] *School of Pharmacy, China Pharmaceutical University;* [b] *School of Traditional Chinese Medicine, China Pharmaceutical University; and* [c] *Center of Drug Discovery, China Pharmaceutical University; Nanjing 210009, P. R. China.*
Received February 24, 2011; accepted March 17, 2011; published online March 29, 2011

$ZCVI_4$-2 is a newly developed furoxan-based nitric oxide-releasing derivative of oleanolic acid. It exhibited strong cytotoxicity against human hepatocellular carcinoma (HCC) *in vitro* and significantly inhibited the growth of HCC tumors *in vivo*. However, its low aqueous solubility and toxicity due to the fast release of nitric oxide (NO) in blood challenged its formulation. In the present investigation, the interaction characteristics of $ZCVI_4$-2 with bovine serum albumin (BSA) were studied by fluorescence spectrometry, synchronous fluorescence spectra and Fourier transform-infrared (FT-IR). It was found that $ZCVI_4$-2 concentration, temperature and pH had significant effect on the interactions. $ZCVI_4$-2 was able to bind BSA with high affinity, low temperature and neutral pH favor the binding. The interaction exhibited to be a spontaneous and exothermic process. $ZCVI_4$-2 was buried in the hydrophobic pocket in subdomain IIB of BSA and the exact binding site was around 3.83 nm in average from Trp^{212}. The NO releasing characteristics of nanocomplexes were compared with $ZCVI_4$-2 solution by Griess Reagent Method. It was found that the release of NO from $ZCVI_4$-2/BSA nanocomplexes was retarded significantly, thus making $ZCVI_4$-2 into a BSA-bound nanocomplexes had the great potential to lower the toxicity due to the absence of organic solvents and surfactants and meanwhile the sustained release of NO.

Key words $ZCVI_4$-2; bovine serum albumin; interaction; nitric oxide release

Human hepatocellular carcinoma (HCC) is one of the leading causes for mortality in the world and there is no effective chemotherapy at present. Therefore, development of new therapeutically effective and low toxic reagents, particularly injectable drugs, will be of great significance.

$ZCVI_4$-2 (Fig. 1) is a newly developed furoxan-based nitric oxide-releasing derivative of oleanolic acid, and has been successfully synthesized as galactosyl derivative 3 of the compound 1 (furoxan-based nitric oxide-releasing derivative of oleanolic acid) by Huang *et al.*[1] As reported previously, it exhibited strong cytotoxicity against HCC *in vitro* and significantly inhibited the growth of HCC tumors *in vivo*, indicating that $ZCVI_4$-2 may be a promising candidate for the treatment of human HCC.[1] However, $ZCVI_4$-2 has a very low aqueous solubility ($<10\,\mu$g/ml at pH 3.0—9.0). The poor solubility of $ZCVI_4$-2 has been a major hindrance in the development of its parenteral dosage forms. In our previous research, the combination of macrogol 15 hydroxystearate (Solutol HS-15), propylene glycol and ethanol was used to improve its solubility successfully to be up to 5 mg/ml. *In vivo* activity evaluation indicated that $ZCVI_4$-2 treatment with 25 mg/kg of $ZCVI_4$-2 enhanced the inhibitory effect on the growth of HCC tumors SMMC-7721 transplanted in nude mice ($p<0.01$ *vs.* treatment with 12.5 mg/kg), and its inhibitory effect was similar to that of 5-FU treatment. The tumor weights in the mice treated with $ZCVI_4$-2 at 12.5 or 25 mg/kg was significantly lower than that from the vehicle-treated controls ($p<0.01$). However, $ZCVI_4$-2 injection displayed obvious toxicity to mice in toxicological studies with a LD_{50} value of 94.1 mg/kg.[1] By comparing the mice survival of $ZCVI_4$-2 suspension with $ZCVI_4$-2 injection, it was inferred that the toxicity of $ZCVI_4$-2 may be attributed firstly to the fast release of nitric oxide (NO) in blood and secondly to the surfactant and organic solvents in the formulation.

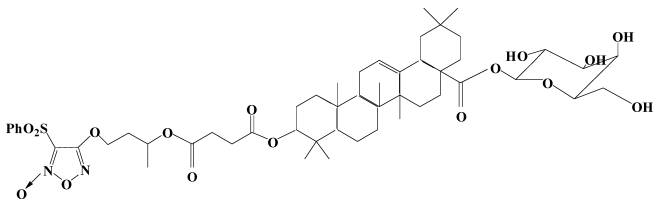

Fig. 1. The Structure Formula of $ZCVI_4$-2

The serum albumin was used frequently for the preparation of nanoparticles because of its excellent water-solubility and biocompatibility. Human serum albumin (HSA) had been successfully bound with paclitaxel and formulated into Abraxane®, the paclitaxel protein-bound particles for injectable suspension. The absence of organic solvents and surfactants significantly improved the clinical safety.[2—5] The key step to prepare the protein (bovine serum albumin (BSA) or HSA)-bound nanocomplex is to determine the rational condition for the binding between drug and protein through interaction study. To date, however, the interaction characteristics, the binding condition for paclitaxel and HSA, the screening process of formulation and technology of Abraxane® were not reported.

To delay the release of the NO, and to lower the toxicity after injection, the serum albumin (BSA) was utilized for the preparation of the surfactant-free serum albumin nanocomplexes of $ZCVI_4$-2 in this study. The main objective of the present study is to study the interaction characteristics between $ZCVI_4$-2 and BSA and then to determine the preparation parameters of $ZCVI_4$-2 BSA-bound injectable nanocomplexes. Moreover, the NO release characteristics of $ZCVI_4$-2/BSA nanocomplexes were also studied to reveal the influence of serum albumin nanocomplexes.

* To whom correspondence should be addressed. e-mail: amicute@163.com; windy1984122@126.com

Experimental

Materials Albumin Bovine V was purchased from Sigma, U.S.A. $ZCVI_4$-2 was synthesized by Center of Drug Discovery of China Pharmaceutical University (Nanjing, China). Sodium Nitrite was purchased from Shanghai Sino Fine Chemical Co., Ltd. (Shanghai, China). *N*-1-Napthylethylenediamine dihydrochloride and sulfanilamide were purchased from Sinopharm Chemical Reagent Co., Ltd. (Shanghai, China). L-Cysteine was purchased from HuaXing Biochemistry Reagent Co., Ltd. (Menzhou, China). Other chemicals were of HPLC or analytical grade.

Methods. The Quenching of Intrinsic Fluorescence of BSA by $ZCVI_4$-2 $ZCVI_4$-2 solutions with concentrations from 0 to 100 μg/ml at an interval of 20 μg/ml were prepared as control groups by dissolving $ZCVI_4$-2 in ethanol and subsequent dilution. Fluorescence scanning of these solutions was conducted at the excitation wavelength of 280 nm, the emission spectra of 250—400 nm were recorded to examine whether the drug and ethanol emit fluorescence when excited by UV light.

$ZCVI_4$-2 solutions with concentrations from 0 to 100 μg/ml at an interval of 20 μg/ml were prepared by diluting $ZCVI_4$-2 ethanol solution (4.0 mg/ml) in two phosphate buffers (pH 3.0 and pH 6.8, 0.01 mol/l); the concentration of BSA in each solution was 0.5 mg/ml. Fluorescence scanning of these samples were carried out at 4 °C, 15 °C, 22 °C and 30 °C respectively as described above to evaluate the influence of temperature and pH environment on the quenching of intrinsic BSA fluorescence.

A series of solutions with pH ranging from 2.13 to 11.76 were prepared, and under each pH, the concentrations of $ZCVI_4$-2 were from 0 to 100 μg/ml at an interval of 20 μg/ml by diluting $ZCVI_4$-2 ethanol solution (4.0 mg/ml) in buffers; the concentrations of BSA in all the solutions were 0.5 mg/ml. Fluorescence scanning of these solutions were conducted were carried out at 30 °C as described above to study the effect of pH on the quenching of BSA intrinsic fluorescence.

Synchronous fluorescence spectrometry of BSA was performed to explore the structural change of BSA caused by $ZCVI_4$-2. The synchronous fluorescence spectra of these solutions above were obtained by setting $\Delta\lambda=15$ nm and $\Delta\lambda=60$ nm, respectively. The excitation and emission slit widths were set at 10.0 nm.

The Quenching Effect of $ZCVI_4$-2 on BSA Fluorescence Intensity The classical relationship often employed to describe the collisional quenching process is the Stern–Volmer equation[6,7]:

$$\frac{F_0}{F}=1+K_q\tau_0[D]=1+K_{sv}[D] \tag{1}$$

Where F_0 and F are the fluorescence intensity in the absence and presence of quencher ($ZCVI_4$-2), K_q is the quenching rate constant of the biomacromolecule (BSA), which reflects the influence of diffusion and collision between the biomacromolecule (BSA) and the fluorescence quencher on the decay rate of fluorescence lifetime of biomacromolecule in the system.[7] The maximum dynamic collision quenching constants of various kinds of quenchers are around $2.0\times10^{10}\,l^{-1}\,mol^{-1}\,s^{-1}$ for biopolymers fluorescence and $7\times10^{9}\,M^{-1}\,s^{-1}$ for protein.[8] τ_0 is the lifetime of the fluorescence in the absence of quencher, and for BSA, τ_0 is around 10.[8,9] $K_{sv}=K_q\times\tau_0$ is the Stern–Volmer quenching constant, K_{sv} indicates the dose–effect relationship between the biomacromolecule (BSA) and fluorescence quencher when the diffusion and collision between them reaches a dynamic equilibrium.[7] [D] is the concentration of the quencher ($ZCVI_4$-2).

Herein, Eq. 1 was applied to determine K_{sv} by a linear regression of the plot of F_0/F against [D]. A linear Stern–Volmer plot is generally indicative of the presence of a single class of fluorophores in a protein, all equally accessibly to the quencher, this also means that only one quenching mechanism (dynamic or static) exists.[10]

For static quenching, when small molecules bind independently to a set of equivalent sites on a macromolecule, the equilibrium between free and bound molecules is described by the Scatchard equation or Binding equation, Eq. 2[11—13]:

$$\log\left[\frac{F_0-F}{F}\right]=\log K_b+n\log[D] \tag{2}$$

Where K_b is the dissociation binding constant which is an indicator of the affinity to the binding site,[13] also reflects the degree of interaction between BSA and $ZCVI_4$-2; n is the number of binding sites per albumin molecule, here it refers to the number of $ZCVI_4$-2 bound to a BSA macromolecule.[14] According to Eq. 2, binding parameters can be obtained by plotting $\log(F_0-F)/F$ *versus* $\log[D]$.[15—17]

Fluorescence Emission of Control Groups To exclude the influence of ethanol and $ZCVI_4$-2 on the fluorescence spectrum of BSA, the fluorescence signals of control groups with $ZCVI_4$-2 solution (0—100 μg/ml) and a fixed amount of ethanol were monitored in the tested excitation and emission wavelength. The results showed that the emission of control groups were negligible, thus ethanol and free $ZCVI_4$-2 did not affect the fluorescence spectrum of BSA.

The Binding Site Estimation The fluorescence intensity of BSA (F_0) and $ZCVI_4$-2 (F) solutions was tested in RF-5301PC-Spectrofluorophotometer (Shimadzu Scientific Instruments, Inc., Japan) at an excitation wavelength of 280 nm and an emission wavelength of 388 nm. UV absorption spectrum of $ZCVI_4$-2 was obtained by scanning $ZCVI_4$-2 solution in a UV spectrophotometer (8453 Visible Spectroscopy, Agilent Technologies, Ltd., U.S.A.) from 300 to 400 nm. Fluorescence emission spectrum of BSA was obtained by fluorescence scanning of BSA solution at an excitation wavelength of 280 nm and emission wavelength of 300—400 nm. The concentrations of BSA and $ZCVI_4$-2 solutions were both 7.4×10^{-6} mol/l. F_0, F, UV absorption spectrum of $ZCVI_4$-2 and fluorescence emission spectrum of BSA were measured under pH from 2.13 to 11.76 to estimate the binding sites under different pH.

According to the Förster theory, the energy transfer efficiency E is defined as following Eq. 3[13,18]:

$$E=1-\frac{F}{F_0}=\frac{R_0^6}{R_0^6+r^6} \tag{3}$$

Here F_0 and F is the fluorescence intensity of donor in the absence and presence of equal amount of accepter ($ZCVI_4$-2) respectively, r is the distance between the donor (Trp^{212} of BSA) and the acceptor ($ZCVI_4$-2), R_0 is the Förster distance (R_0), which is the critical energy-transfer distance and can be calculated using Eq. 4[13,19]:

$$R_0^6=8.8\times10^{-25}K^2N^{-4}\Phi J \tag{4}$$

Where K^2 is the spatial orientation factor of the dipole, N the refractive index of the medium, Φ the fluorescence quantum yield of the donor, and J is the overlap integral of the fluorescence emission spectrum of the donor and the absorption spectrum of the acceptor was given by Eq. 5[13,19]:

$$J=\frac{\int_0^\infty F(\lambda)\varepsilon(\lambda)\lambda^4 d\lambda}{\int_0^\infty F(\lambda)d\lambda} \tag{5}$$

Here $F(\lambda)$ is the fluorescence intensity of the fluorescence donor at wavelength λ and $\varepsilon(\lambda)$ is the molar absorptivity of the acceptor at wavelength λ. $F(\lambda)$ and $\varepsilon(\lambda)$ were determined by analysis of fluorescence spectroscopy and ultraviolet spectroscopy using OriginPro 7.5 software.

Preparation of $ZCVI_4$-2 BSA-Bound Nanocomplexes Five milligrams per milliliters BSA solution was prepared by dissolving BSA in 50 mmol/l phosphate buffer solution at pH 6.8. $ZCVI_4$-2 stock ethanolic solution (1.06 mg/ml) was then added to BSA solution (4 °C) at a constant rate of 0.1 ml/min to obtain nanocomplexes ($C_{BSA}=16$ mg/ml, $C_D=5.56$ mg/ml). The particle size analysis was performed by photon correlation spectroscopy (PCS) using a Zetasizer 3000 (Malvern Instruments, Malvern, U.K.). Each sample was measured at 25 °C in triplicate. PCS yields the volume weighted mean particle size and the polydispersity index (PI) of the liquid nanocomplexes.

Preparation of BSA-Loaded $ZCVI_4$-2 Nanocomplexes with Freeze-Drying Protectant Based on the preliminary screening, the combination of 3% mannitol and 4% sucrose was added to BSA-loaded $ZCVI_4$-2 nanocomplexes as the lyoprotectant to investigate the influence of lyoprotectant on the release of NO from $ZCVI_4$-2.

Fourier Transform-Infrared (FT-IR) Study The solid nanocomplex product was obtained by freeze-drying the binary solution of BSA (0.5 mg/ml) and $ZCVI_4$-2 (0.1 mg/ml). The physical mixture was gained by milling equal amount of BSA and $ZCVI_4$-2. Infrared spectra of all samples were recorded on a Bruker Tensor 27 Fourier transform infrared spectrometer (Bruker Optics Inc., Germany).

Nitric Oxide Measurement *in Vitro* The NO measurement was performed to investigate the potential retarding effect of BSA binding on the NO releasing of $ZCVI_4$-2 by comparison with $ZCVI_4$-2 solution. $ZCVI_4$-2 solution was prepared in 0.2% Solutol HS-15, using 50 mmol/l phosphate buffer solution (pH 6.8) containing 5% ethanol as solvent. Reconstituted

nanocomplex was prepared by reconstitute the lyophilized product in 50 mmol/l phosphate buffer solution (pH 6.8) to evaluate the effect of lyophilization on the NO releasing. The control group of each sample contained all the components except for the drug. The concentration of $ZCVI_4$-2 in each sample was 0.1 mg/ml, and ethanol was 5%. The concentration of BSA in BSA contained samples was 5 mg/ml.

The characteristics of NO release were studied by using the Griess reaction.[20—23] Briefly, 5 mmol/l L-cysteine was dissolved in all the samples, and the samples immediately were put into the oven set at 37 °C for 30 min. Two milliliters aliquots of each sample was mixed with 0.5 ml aliquots of Griess reagent (4% sulphanilamide; 0.4% *N*-naphtylethylendiamine dihydrochloride; 10% H_3PO_4, w/v) every other 30 to 120 min and incubated at room temperature for 10 min to form an azo-dye. Absorbance was monitored at 540 nm using a UV spectrophotometer and the amount of NO was quantified with $NaNO_2$ as a standard (the calibration curve was linear over the concentrations range from 0.12 to 1.6 μg/ml (r=0.9999)). The capacity to release NO was expressed as the concentration of NO^{2-}.

Results and Discussion

The Influence of Temperature on the Quenching of Intrinsic Fluorescence of BSA by $ZCVI_4$-2 Fluorescence quenching spectra of BSA solutions (in pH 3.0 and pH 6.8) changed with temperature (Fig. 2). The addition of drug generally had a quenching effect on BSA fluorescence, which was seen in the whole temperature range investigated when pH was 6.8 and at 4 °C and 15 °C when pH was 3.0. Nevertheless, at pH 3.0 (22, 30 °C), the BSA fluorescence spectrum was sensitized following the addition of drug.

The fluorescence data of samples at different temperatures were analyzed by Stern–Volmer equation, and the Scatchard equation, the results were listed in Table 1.

The correlation coefficients were larger than 0.90, indicating that the interaction between $ZCVI_4$-2 and BSA agreed well with the Stern–Volmer equation and binding equation. A linear Stern–Volmer plot is generally indicative of a single class of fluorophores in a protein, all equally accessibly to the quencher, which also means the presence of only one quenching mechanism (dynamic or static).[10]

As presented in Table 1, at pH 6.8, a negative dependence of K_q on temperature was observed in the quenching of BSA fluorescence by $ZCVI_4$-2, and $K_q > 2.0\times10^{10}$ l·mol^{-1}·s^{-1} (the maximum dynamic collision quenching constant of various kinds of quenchers for biopolymers fluorescence), it can be concluded that the nature of quenching is not dynamic but more likely static.

At both pH (Table 1), the K_q values were at the order of magnitude of 10^{11} M^{-1}·s^{-1}, far above the maximum values expected for dynamic quenching of residues in proteins (7×10^9 M^{-1}·s^{-1}).[8] The result suggests the quenching mechanism is static. It was found that both the binding constant K_b and 'n' decreased with the increase in temperature, resulting in reduction of the stability of the $ZCVI_4$-2/BSA complexes. Therefore low temperature is preferred for $ZCVI_4$-2/BSA binding.

Types of Interaction Force between $ZCVI_4$-2 and BSA Considering the dependence of binding constant on temperature, a thermodynamic process was considered to be responsible for the formation of the nanocomplexes. Therefore, the temperature-dependent thermodynamic parameters were analyzed in order to further characterize the interacting forces between $ZCVI_4$-2 and BSA. The interaction forces between a small molecule and macromolecule generally include hydrogen bonding, van der Waals forces, electrostatic forces and

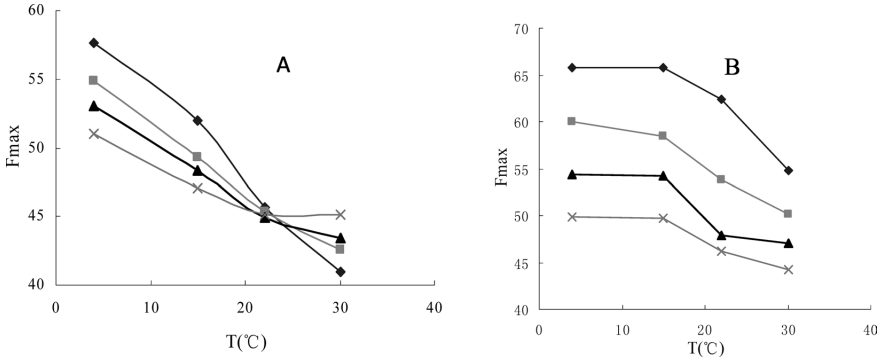

Fig. 2. The Influence of Temperature and $ZCVI_4$-2 Concentration (C_D) on Quenching of Intrinsic Fluorescence of BSA by $ZCVI_4$-2 at pH 3.0 (A) and pH 6.8 (B)

(×) C_D=60 μg/ml, (▲) C_D=40 μg/ml, (■) C_D=20 μg/ml, (◆) C_D=0 μg/ml.

Table 1. Stern–Volmer Constant, Quenching Rate Constant, Binding Constant and the Number of Binding Sites at pH 3.0 and pH 6.8 at Different Temperatures

pH	Temp. (°C)	Stern–Volmer			Binding equation		
		R^2	K_{sv} (l/mol)	K_q (l/mol·s)	R^2	K_b (l/mol)	n
3.0	4	0.9782	1546.1	$1.8461\cdot10^{11}$	0.9957	423.8	0.8366
	15	0.9982	1865.4	$1.5654\cdot10^{11}$	0.9817	377.1	0.7741
	22	0.9374	1904.6	$1.5296\cdot10^{11}$	0.953	370.2	0.7201
	30	0.9949	2197.0	$1.4970\cdot10^{11}$	0.9765	279.7	0.6803
6.8	4	0.9988	4775.3	$4.7753\cdot10^{11}$	0.9964	14547.9	1.1188
	15	0.9982	4327.6	$4.3276\cdot10^{11}$	0.9955	3390.2	0.9749
	22	0.9587	3995.9	$3.9959\cdot10^{11}$	0.9893	172.3	0.8535
	30	0.9853	2469.6	$2.4696\cdot10^{11}$	0.9966	416.5	0.8044

hydrophobic interaction forces. The characteristic signs of the thermodynamic parameters were reported to be associated with the various individual kinds of interaction forces between a small molecule and macromolecule (BSA).[24] It was also concluded that the only contributions to positive entropy and enthalpy changes arise from ionic and hydrophobic interactions and the only sources of negative enthalpy and entropy changes arise from van der Waals and hydrogen-bond in low dielectric media. The thermodynamic parameters were evaluated using Van't Hoff equation,[12,17] The results obtained are shown in Table 2.

The negative values of ΔG reveal that the interaction process is spontaneous. A negative ΔH value indicates an exothermic process, and low temperature is helpful for the binding process. In this case, high dielectric media aqueous buffers were used, so the interaction forces between $ZCVI_4$-2 and BSA were van der Waals forces.

The Effect of Temperature on the Stability of the $ZCVI_4$-2/BSA Nanocomplexes Fluorescence strength of BSA decreased with the increase of temperature by about 29% (0 μg/ml), 22% (20 μg/ml), 17% (40 μg/ml), 9% (60 μg/ml) at pH 3.0, and about 16% (0 μg/ml), 15% (20 μg/ml), 10% (40 μg/ml), 5% (60 μg/ml) at pH 6.8 (Fig. 2). With the increase of $ZCVI_4$-2 concentration, BSA fluorescence became less dependent on temperature, the stability of the $ZCVI_4$-2/BSA nanocomplexes increased. Since the main factor in temperature-related denaturation is the breaking of the hydrogen bonds, the improved thermo-stability may stem from the hydrogen bonds formed between $ZCVI_4$-2 and the $-NH_2$ or OH groups in BSA. Moreover, the lack of dependence on temperature at higher $ZCVI_4$-2/BSA molar ratio leads us to hypothesize that there are additional stabilization factors between the $ZCVI_4$-2 and BSA, such as van der Waals forces.[25,26]

When comparing the stability of the nanocomplex at two given pH values, we found that the complex showed less temperature dependence at pH 6.8 than that at pH 3.0, thus the nanocomplex was more stable at pH 6.8. This could be explained by the conformational change from pH 6.8 to 3.0, which would be further discussed in the following text. At neutral pH, the macromolecule BSA was tightly folded. While at lower pH, it became only loosely connected, and was more sensitive to the variation of the temperature.

Effect of $ZCVI_4$-2 Concentration on the Quenching of Intrinsic Fluorescence of BSA under a Series of pHs With the increase of $ZCVI_4$-2 concentration, the fluorescence quenching of BSA increased in the pH ranges investigated, meanwhile, a blue shift happened to the wavelength of maximum emission (Fig. 3). Except for samples at pH 3.15, a blue shift (6—10 nm) was observed in the maximum emission wavelength of the rest samples. Measuring the peak emission shift is a commonly used method to study the environment of tryptophan. The shift in the peak of emission corresponds to the changes of the polarity around chromophore molecule. The blue shift indicated a decrease in polarity around the tryptophan residues and an increased hydrophobicity.[11,26]

K_b and 'n' were calculated using the Binding equation, Eq. 2, and the results are listed in Table 3. The correlation coefficients were larger than 0.90, indicating that the interaction between $ZCVI_4$-2 and BSA agreed well with the site binding model (Eq. 2). Both K_b and 'n' reach a maximum at pH 8.78, the second largest value occurred at pH 5.08.

With the increase of pH, several transitions appeared for serum albumins: acid-leaded expansion to fastmigrating at pH 2.5—3.5 (expanded-F), fastmigrating to normal at pH 3.5—4.5 (F–N) and normal to base at pH 6.5—8.5 (N–B).[27—29] Generally, under neutral pH, two spherical parts of the BSA were closely combined. When pH is lowered, the two parts become loosely connected,[28] helical structure under the neutral pH transformed to random coil structure under low pH.

In the pH range of 2.0—3.5, BSA solution is in 'expanded' form. The tryptophan residues transferred into a more hydrophobic environment of the BSA molecule, meanwhile, the hydrophilicity of the whole BSA molecule increased,[30] which was coincide with the following results.

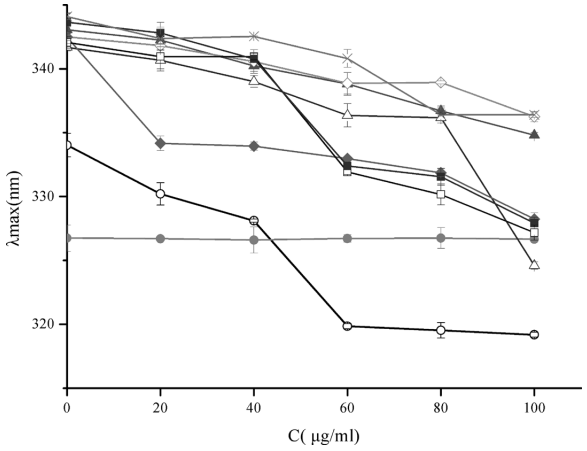

Fig. 3. The Variation of λ_{max} with the Change of the $ZCVI_4$-2 Concentration (C_D) at pH 2.13—11.76

(○) pH 2.13, (●) pH 3.15, (△) pH 5.08, (▲) pH 6.26, (◇) pH 7.45, (◆) pH 8.78, (□) pH 9.50, (■) pH 10.50, (×) pH 11.76.

Table 2. The Thermodynamic Parameters and Types of Interaction between $ZCVI_4$-2 and BSA at pH 3.0 and pH 6.8 at Different Temperatures

pH	Temp. (°C)	ΔH (kJ/mol)	ΔS (kJ/mol·K)	ΔG (kJ/mol)	Interaction type
3.0	4	$-1.03\cdot10^5$	−320.8	$-1.39\cdot10^4$	van der Waals
	15	$-7.66\cdot10^5$	−2695.3	$-1.04\cdot10^4$	van der Waals
	22	$-1.358\cdot10^5$	−1714	$-0.93\cdot10^4$	van der Waals
6.8	4	$-8.78\cdot10^4$	−237	$-2.21\cdot10^4$	van der Waals
	15	$-3.01\cdot10^5$	−977	$-1.95\cdot10^4$	van der Waals
	22	$-8.20\cdot10^4$	−321	$-1.26\cdot10^4$	van der Waals

Table 3. The Influence of pH on the Binding of $ZCVI_4$-2 to BSA

pH	$\lg(F_0/F-1)=\lg k_b+n\lg[D]$		
	R^2	K_b (l/mol)	n
2.13	0.9670	71.17	0.6301
3.15	0.9755	3250.13	0.9739
5.08	0.9909	87902.25	1.3078
6.26	0.9902	35950.09	1.2318
7.45	0.9938	11641.26	1.0924
8.78	0.9984	98310.52	1.3169
9.50	0.9965	46881.00	1.2420
10.50	0.9875	6581.00	1.0470
11.76	0.9903	161.60	0.6787

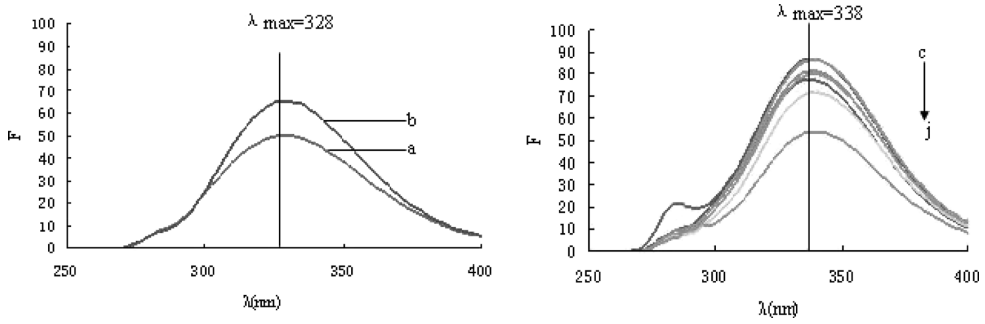

Fig. 4. The Fluorescence Spectra when C_{BSA}=0.5 mg/ml, C_D=0 μg/ml, pH=2.13—11.76
(a→j) pH 2.13, pH 3.15, pH 3.98, pH 5.08, pH 6.26, pH 7.45, pH 8.78, pH 9.50, pH 10.50, and pH 11.76.

With the decrease of pH from neutral to pH 2 and pH 3, the wavelength of maximum emission both decreased from 338 to 328 nm, resulting in a blue shift of 10 nm (Fig. 4), which indicated that the polarity around the tryptophan residues was decreased and the hydrophobicity was increased.[11,31] The hydrophobic region where tryptophan residues located was the very location $ZCVI_4$-2 bound to. When BSA was in the 'expanded' form, there was more hindrance for $ZCVI_4$-2 to reach the binding position for it was more deeply buried under this pH range. Nevertheless, the $ZCVI_4$-2/BSA nanocomplexes showed superior solubility under this pH range, because of the increase of the hydrophilicity of the whole BSA molecule. The 'K_b' and 'n' of samples under pH 2.13 and pH 3.15 were relatively low, as shown in Table 3, and more $ZCVI_4$-2 can be solubilized by BSA solution in this pH range than at other pHs (data not shown), which coincides with the theory in literatures.[11,30,31]

Relatively high 'K_b' and 'n' were observed as shown in Table 3 when BSA was in native or 'N' form (about pH 5.0—7.0).[28] In this pH range, more tryptophan residues were exposed to a hydrophilic environment, which made it easier for $ZCVI_4$-2 to reach the binding site.

The maximum 'K_b' and 'n' values were obtained under pH 8.78. When the pH value is above 8.0, the BSA molecule undergoes expansion and the conformation changes to the basic form.[31—33] It was reported that the N–B transition causes strengthening of ligand binding to subdomain IIB (where the tryptophan residues located)[27,29,32,34] which was also demonstrated by 'K_b' and 'n' values in Table 3. Above pH 8, all basic groups become deprotonated and all carboxyl groups become negatively charged, thus amino acids deprotonated. The breaking of salt bridges between domain I and domain III also contributes to the phenomenon.[28—30,35] Compared to 'N' form, the fluctuations of the main chain of the 'B' form are increased, the thermal stabilities were greatly reduced.[29,34,35] This might account for the fact that $ZCVI_4$-2 did not exhibit high solubility in BSA solution under alkaline pH (data were not provided).

The Binding Site According to Förster's non-radiative energy transfer theory,[36—38] the energy transfer would happen under the following conditions[39]: (i) the donor(Trp^{212} of BSA) can produce fluorescence light, (ii) the fluorescence emission spectrum of the donor and UV absorption spectrum of the acceptor ($ZCVI_4$-2) have enough overlap and (iii) in all case, the distance between the donor and the acceptor is at least 3.63 nm, and up to 4.24 nm.[18] The fluorescence quenching of BSA after binding with $ZCVI_4$-2 indicated that the energy transfer between $ZCVI_4$-2 and BSA had occurred. The overlap of the UV absorption spectrum of $ZCVI_4$-2 with the fluorescence emission spectrum of BSA is shown in Fig. 5.

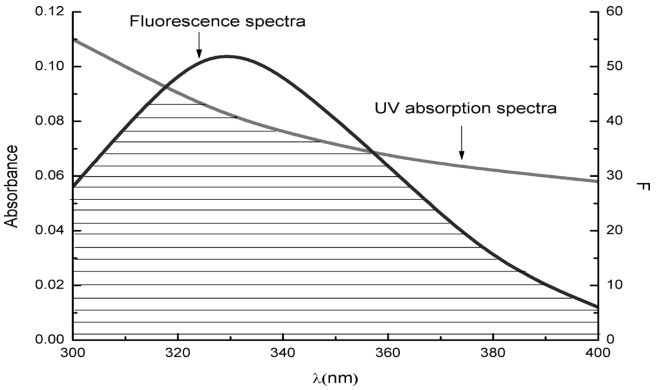

Fig. 5. The Overlap of Fluorescence Spectra of BSA with the UV Absorption Spectra of $ZCVI_4$-2

Table 4. The Variation of the Distance between $ZCVI_4$-2 and the Trp^{212} Residue (r) with the Change of pH (2.13—11.76)

pH	F/F_0	J ($cm^3 \cdot l/mol$)	R_0 (nm)	r (nm)	Average (nm)
2.13	0.834	$1.27 \cdot 10^{-14}$	3.17	4.15	3.83±0.14
3.15	0.762	$1.27 \cdot 10^{-14}$	3.17	3.85	
5.08	0.732	$1.30 \cdot 10^{-14}$	3.18	3.76	
6.26	0.747	$1.29 \cdot 10^{-14}$	3.17	3.8	
7.45	0.728	$1.28 \cdot 10^{-14}$	3.17	3.73	
8.78	0.719	$1.28 \cdot 10^{-14}$	3.17	3.71	
9.5	0.734	$1.27 \cdot 10^{-14}$	3.16	3.74	
10.5	0.755	$1.27 \cdot 10^{-14}$	3.16	3.81	
11.76	0.781	$1.27 \cdot 10^{-14}$	3.16	3.91	

The distance (r) between the donor (Trp^{212} of BSA) and the acceptor ($ZCVI_4$-2) can be calculated using Eqs. 3—5 and the results were presented in Table 4.

The distance between $ZCVI_4$-2 and the Trp^{212} residue (r) was around 3.83 nm in average, and it was little influenced by the pH change. Therefore, it can be concluded that, $ZCVI_4$-2 was buried in the hydrophobic pocket in subdomain IIB of BSA, where the Trp^{212} residue located. And the exact binding site was about 3.83 nm from Trp^{212}.

Analysis of BSA Conformation after $ZCVI_4$-2 Binding Although it was found out that it was the binding of $ZCVI_4$-2

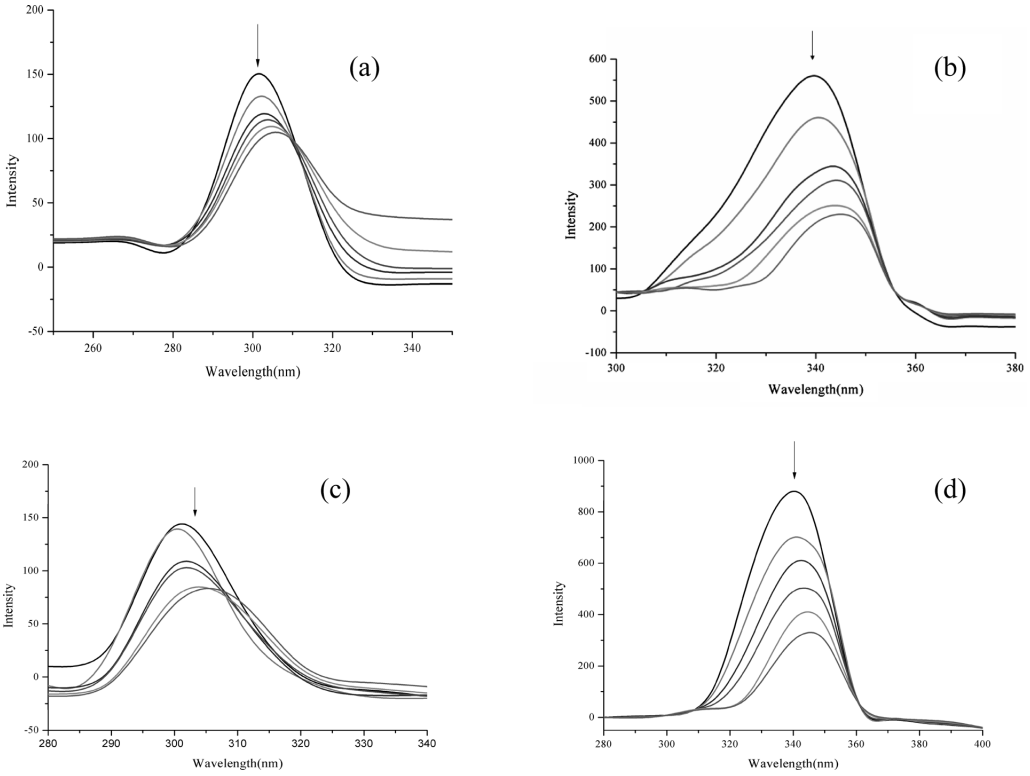

Fig. 6. The Synchronous Fluorescence Spectra of BSA at pH 3.0/$\Delta\lambda$=15 nm (a), pH 3.0/$\Delta\lambda$=60 nm (b), pH 6.8/$\Delta\lambda$=15 nm (c) and pH 6.8/$\Delta\lambda$=15 nm (d)
Shown as the arrow, from up to down: C_D=0 μg/ml; 20 μg/ml; 40 μg/ml; 60 μg/ml; 80 μg/ml; 100 μg/ml.

to BSA that caused the fluorescence quenching of BSA, it is still unclear whether the binding affects the conformation and/or the microenvironment of BSA. To further verify the binding of $ZCVI_4$-2 to BSA and to explore the structural change of BSA after the addition of $ZCVI_4$-2, FT-IR and the synchronous fluorescence spectra of BSA with various amounts of $ZCVI_4$-2 were measured (Fig. 6).

In the synchronous spectra, the sensitivity associated with fluorescence is maintained, while offers several advantages: spectral simplification, spectral bandwidth reduction and avoiding different disturbing effects.[39—41] The intrinsic fluorescence of albumins results from the tryptophan and tyrosine residues, and the normal emission spectra of tryptophan and tyrosine residues are overlap, while the synchronous fluorescence spectra is able to distinguish them.[42—44] When the $\Delta\lambda$ between excitation wavelength and emission wavelength is fixed at 15 or 60 nm, the synchronous fluorescence will provide information on the microenvironment of tyrosine residues or tryptophan residues respectively.[43,44]

As can be seen from Fig. 6, after the addition of $ZCVI_4$-2, a stronger fluorescence quenching effect of tryptophan residues (Fig. 6b, d) is observed compared with that of the tyrosine residues (Figs. 6a, c). This difference indicated that the binding site of $ZCVI_4$-2 is more close to tryptophan residues. BSA consists of 582 amino acid residues forming a single polypeptide with well-known sequence, which contains three homologous α-helices domains (i—iii). Each domain is divided into two sub-domains (A and B). The adherence of two sub-domains with their grooves towards each other forms a domain, and three of such domains make up an albumin molecule.[45,46] BSA has two tryptophan residues (Trp^{135} and Trp^{214}) located in subdomains IA and IIA, respectively.[43,47] A large hydrophobic cavity is present in the IIA sub-domain, and a wide variety of arrangements can take place in this sub-domain. Trp214 is deeply buried in sub-domain IIA where the highly hydrophobic molecule $ZCVI_4$-2 can better penetrate, whereas Trp^{135} is located in sub-domain IA which is more exposed to a hydrophilic environment. Therefore, it can be inferred that the primary binding target of $ZCVI_4$-2 is sub-domain IIA of BSA where Trp^{214} is located. This conclusion is in accordance with the results on the previous part. Moreover, remarkable red shift of maximum emission wavelength of tryptophan residue and the tyrosine residue were observed upon the addition of $ZCVI_4$-2, That red shift indicates that the conformation of BSA is changed and tryptophan residues are placed in a more hydrophilic environment, resulting in a increase of polarity in the fluorophore environment, and more exposed to the aqueous environment.[43,44] Moreover, following the addition of $ZCVI_4$-2, fluorescence quenching effect of tryptophan residues (Figs. 6b, d) and tyrosine residues (Figs. 6a, c) are both stronger in pH 6.8 than that of in pH 3.0, also showing that binding effect of $ZCVI_4$-2 to tryptophan residues and tryptophan residues of BSA in pH 6.8 is stronger than that in pH 3.0, then to indicate that the environment of pH 6.8 is more helpful for the binding course.

Figure 7 showed the FT-IR spectra of the physical mixture and the nanocomplex of $ZCVI_4$-2 and BSA. Usually the amide I band occurs in the region of 1600—1700 cm^{-1} and amide II band occurs near 1548 cm^{-1}. Amide I band is more sensitive to the protein conformation changes than amide II.[48,49] Figure 7 illustrated the shifts in the peak of amide band. For physical mixture and $ZCVI_4$-2-BSA nanocomplex, the amide I occurred at 1654.84 cm^{-1} and 1649.84 cm^{-1}, re-

spectively. A difference of 5 nm was observed between the physical mixture and the nanocomplex. The shift of the amide II was negligible (less than 1 nm). Bases on the results, we proposed that the secondary and tertiary structure of BSA were affected by the binding of $ZCVI_4$-2 to BSA.

The Characteristics of Nitric Oxide Release To evaluate nitric oxide release from $ZCVI_4$-2 in different forms, Griess Reagent Method was applied. Each of these experiments was performed in triplicate. The NO release profiles were shown in Fig. 8 and the average release rate was calculated and listed in Table 5. The difference factor (f_1) and similarity factor (f_2) were used to compare the release profiles. The similarity factor has been adopted by the Center for Drug Evaluation and Research (FDA) and Human Medicines Evaluation Unit of European Agency for the Evaluation of Medicinal Products (EMEA), as a criterion for the assessment of the similarity between two release profiles. Two profiles would be considered similar if f_1 value is lower than 15 (0—15) and f_2 value is higher than 50 (50—100).[50] The f_1 value and f_2 value were listed in Table 5.

$$f_1 = \left\{ \frac{\sum_{t=1}^{n} \left| R_t - T_t \right|}{\sum_{t=1}^{n} R_t} \right\} \times 100\% \quad (6)$$

$$f_2 = 50 \log 10 \left\{ \left[1 + \frac{1}{n} \sum_{t=1}^{n} W_t (R_t - T_t)^2 \right]^{-0.5} \times 100 \right\} \quad (7)$$

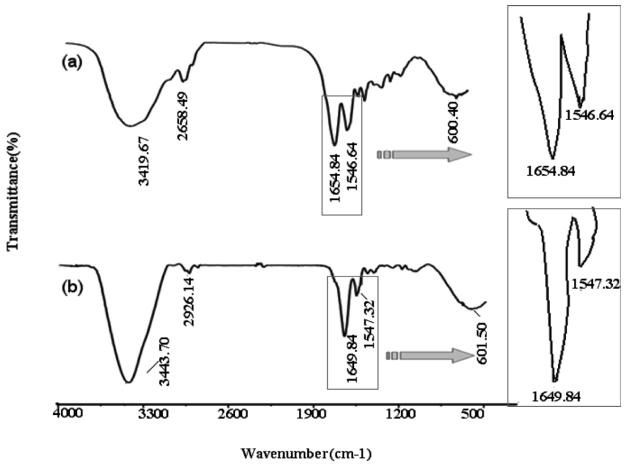

Fig. 7. FT-IR Spectra of the Physical Mixture (a) and the Nanocomplex (b) of $ZCVI_4$-2 and BSA

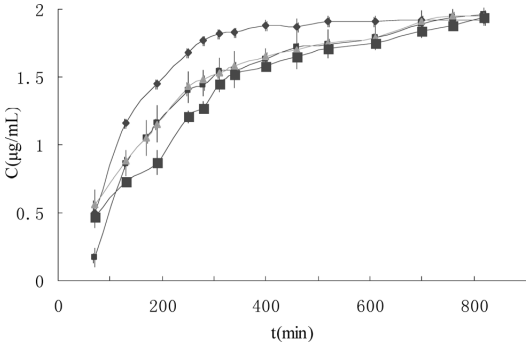

Fig. 8. Release Profiles of Nitric Oxide of Solution and Nanocomplexes

Each value represents mean from six experiments. (◆) $ZCVI_4$-2 solution, solubilized by solutol HS-15, (●) $ZCVI_4$-2 BSA-bound nanocomplex, (▲) $ZCVI_4$-2 BSA-bound nanocomplex containing freeze-drying protectant, (■) Lyophilized $ZCVI_4$-2 BSA-bound nanocomplex.

The results showed that the NO release was significantly retarded when $ZCVI_4$-2 was in a nanocomplex form (sample B—D in the Table 5, Fig. 8) compared to the solution form (sample A in Table 5, Fig. 8). The NO was completely released within 310 min in the solution and 700 min in the nanocomplex form. Correspondently, the rate of NO release from solution was much faster than from nanocomplex (Table 5). The P (t-test), f_1 and f_2 values showed that there was significant difference in NO release between the solution sample (A) and the nanocomplex samples (B—D), but the difference among the nanocomplex samples (B—D) was not significant. The increase of particle size in aqueous environment and during lyophilization had no significant effect on the release of NO (Table 5). These demonstrated that the $ZCVI_4$-2/BSA nanocomplexes were suitable for the sustained release of NO, and consequently had the potential to reduce the toxicity of $ZCVI_4$-2. As mentioned previously, $ZCVI_4$-2 was buried in the hydrophobic region of the BSA when the nanocomplexes formed. BSA was a highly hydrophilic macromolecule, while $ZCVI_4$-2 was a highly hydrophobic small molecule. When the latter was inserted into the hydrophilic pocket of the former, the hydrophobicity of the resulting complex fell between the two of them. The mechanism of NO release from furoxan groups was the nucleophilic attack of RS^- on furoxans.[6,8] Here, L-cysteine acted as a nucleophilic attacker, the NO release occurred only when L-cysteine reached the furoxan group of $ZCVI_4$-2. The formation of nanocomplexes played an important role in hindering the L-cysteine from reaching the group, thus delaying the release of NO from $ZCVI_4$-2.

Conclusion

By investigating the interaction characteristics between BSA and $ZCVI_4$-2, the key preparation parameters of $ZCVI_4$-

Table 5. Particle Size and Nitric Oxide Release Characteristics of $ZCVI_4$-2 Solution and Nanocomplexes

Sample	Particle size (nm)	Release rate (μg/ml·min)		P (t-test)	f_1	f_2	Difference
A	—	0.004977	A and B	0.00058	17.12	41.50	Yes
B	97	0.00255	B and C	0.40416	3.97	60.42	No
C	151	0.002453	C and D	0.98223	3.46	60.40	No
D	183	0.002452	A and D	0.00011	20.07	36.06	Yes

A: $ZCVI_4$-2 solution, solubilized by solutol HS-15. B: $ZCVI_4$-2 BSA-bound nanocomplex. C: $ZCVI_4$-2 BSA-bound nanocomplex containing freeze-drying protectant. D: Lyophilized $ZCVI_4$-2 BSA-bound nanocomplex.

2/BSA nanocomplexes were determined in the study. At suitable temperature and pH, the spontaneous interaction was in favor of the formation of nanocomplex, where $ZCVI_4$-2 was buried in the hydrophobic pocket in subdomain IIB of BSA and the exact binding site was about 3.83 nm from Trp^{212}. The BSA bound formation of nanocomplex may be used as a novel and template approach to sustain the release of NO from the serials of nitric oxide-releasing derivatives of oleanolic acid, which have the similar low solubility and NO release properties as $ZCVI_4$-2.[1)]

Acknowledgements The authors thank "Scientific and Technological Major Special Project-Significant creation of New Drugs (NO. 2009ZX09103-090) in the Eleventh Five-Year Plan," "The Technology Platform for New Formulation and New DDS, Important National Science and Technology Specific Projects (No. 2009ZX09310-004)" and "Natural Science Projects of Jiang Su Province (No: SBK20080571)" for financial supports.

References

1) Huang Z. J., Zhang Y. H., Zhao L., Jing Y. W., Lai Y. S., Zhang L. Y., Guo Q. L., Yuan S. T., Zhang J. J., Chen L., Peng S. X., Tian J. D., *Org. Biomol. Chem.*, **8**, 632—639 (2010).
2) Ibrahim N. K., Desai N., Legha S., Soon-Shiong P., Theriault R. L., Rivera E., Esmaeli B., Ring S. E., Bedikian A., Hortobagyi G. N., Ellerhorst J. A., *Clin. Cancer Res.*, **8**, 1038—1044 (2002).
3) Falciani M., U.S. Patent 2001/0046961 (2001).
4) Micha J. P., Goldstein B. H., Birk C. L., *Gynecol. Oncol.*, **100**, 437—438 (2006).
5) Karmali P. P., Kotamraju V. R., Kastantin M., Black M., Missirlis D., Tirrell M., Ruoslahti E., *Nanomedicine*, **5**, 73—82 (2009).
6) Birks J. B., *J. Lumin.*, **1—2**, 154—165 (1970).
7) Wen X. D., Li P., Qian Z. M., Yang R., *Acta Chim. Sinica*, **65**, 421—429 (2007).
8) Wu T. Q., Wu Q., Guan S. Y., Su H. X., Cai Z. J., *Biomacromolecules*, **8**, 1899—1906 (2007).
9) Xiao J. B., Chen J. W., Cao H., Ren F. L., Yang C. S., Chen Y., Xu M., *J. Photoch. Photobio. A*, **191**, 222—227 (2007).
10) Soares S., Mateus N., Freitas V., *J. Agric. Food Chem.*, **55**, 6726—6735 (2007).
11) Congdon R. W., Muth G. W., Splittgerber A. G., *Anal. Biochem.*, **213**, 407—413 (1993).
12) Zhao H., Ge M., Zhang Z., Wang W., Wu G., *Spectrochim. Acta A*, **65**, 811—817 (2006).
13) Jiang M., Xie M.-X., Zheng D., Liu Y., Li X.-Y., Chen X., *J. Mol. Struuct.*, **692**, 71—80 (2004).
14) Gong A. Q., Zhu X. S., Hu Y. Y., Yu S. H., *Talanta*, **73**, 668—673 (2007).
15) Xiao J. B., Shi J., Cao H., Wu S. D., Ren F. L., Xu M., *J. Pharm. Biomed. Anal.*, **45**, 609—615 (2007).
16) Han X. L., Mei P., Liu Y., Xiao Q., Jiang F. L., Li R., *Spectrochim. Acta A*, **74**, 781—787 (2009).
17) Kandagal P. B., Seetharamappa J., Ashoka S., Shaikh S. M., Manjunatha D. H., *Int. J. Biol. Macromol.*, **39**, 234—239 (2006).
18) van de Weert M., *J. Fluoresc.*, **20**, 625—629 (2010).
19) Xiao J., Wei X., Wang Y., Liu C., *Spectrochim. Acta A*, **74**, 977—982 (2009).
20) Turnbull C. M., Cena C., Fruttero R., Gasco A., Rossi A. G., Megson I. L., *Br. J. Pharmacol.*, **148**, 517—526 (2006).
21) Green L. C., Wagner D. A., Glogowski J., Skipper P. L., Wishnok J. S., Tannenbaum S. R., *Anal. Biochem.*, **126**, 131—138 (1982).
22) Feelisch M., Schönafinger K., Noack E., *Biochem. Pharmacol.*, **44**, 1149—1157 (1992).
23) Ferioli R., Folco G. C., Ferretti C., Gasco A. M., Medana C., Fruttero R., Civelli M., Gasco A., *Br. J. Pharmacol.*, **114**, 816—820 (1995).
24) Ross P. D., Subramanian S., *Biochemistry*, **20**, 3096—3102 (1981).
25) Sulkdwska A., Maciazek M., Rownicka J., Bojkd B., Pentak D., Sutkdwski W. W., *J. Mol. Struct.*, **8**, 834—836, 162—169 (2007).
26) Wang N., Ye L., Yan F. F., Xu R., *Int. J. Pharm.*, **351**, 55—60 (2007).
27) Callis P. R., *Method Enzymol.*, **278**, 113—150 (1997).
28) Khan M. Y., *Biochem. J.*, **236**, 307—310 (1986).
29) Liang H., *J. Guangxi Normal Univsity*, **12**, 54—59 (1994).
30) Shcharbin D., Klajnert B., Bryszewska M., *J. Biomat. Sci. Polym. E*, **16**, 1081—1093 (2004).
31) Wei X. F., Ding X. M., Liu H. Z., *Spectroscopy and Spectral Analsis*, **20**, 556—559 (2000).
32) Era S., Itoh K. B., Sogami M., Kuwata K., Iwama T., Yamada H., Watari H., *J. Pept. Res.*, **35**, 1—11 (1990).
33) Bos O. J., Labro J. F., Fischer M. J., Wilting J., Janssen L. H., *J. Biol. Chem.*, **264**, 953—959 (1989).
34) Shcharbin D., Klajnert B., Mazhull V., Bryszewska M., *J. Fluoresc.*, **13**, 519—524 (2003).
35) Kosa T., Maruyama T., Sakai N., Yonemura N., Yahara S., Otagiri M., *Pharm. Res.*, **15**, 592—598 (1997).
36) Wu P., Brand L., *Anal. Biochem.*, **218**, 1—13 (1994).
37) Berde C. B., Hudson B. S., Simoni R. D., Sklar L. A., *J. Biol. Chem.*, **254**, 391—400 (1979).
38) Mahesha H. G., Singh S. A., Srinivasan N., Appu Rao A. G., *FEBS J.*, **273**, 451—467 (2005).
39) Cui F. L., Cui Y. R., Luo H. X., Yao X. J., Fan J., Lu Y., *Biopolymers*, **83**, 170—181 (2006).
40) Zhang H. X., Huang X., Zhang M., *J. Fluoresc.*, **18**, 753—760 (2008).
41) Lu J. Q., Jin F., Sun T. Q., Zhou X. W., *Int. J. Biol. Macromol.*, **40**, 299—304 (2007).
42) Yang Y., Hua Q., Fan Y., Shen H., *Spectrochim. Acta A*, **69**, 432—436 (2007).
43) Xiang G. H., Tong C. L., Lin H. Z., *J. Fluoresc.*, **17**, 512—521 (2007c).
44) Zhang Y. Z., Zhou B., Liu Y. X., Zhou C. X., Ding X. L., Liu Y., *J. Fluoresc.*, **18**, 109—118 (2008b).
45) Kragh-Hansen U., *Pharmacol. Rev.*, **33**, 17—53 (1981).
46) Petitpas I., Grüne T., Bhattacharya A. A., Curry S., *J. Mol. Biol.*, **314**, 955—960 (2001).
47) Labieniec M., Gabryelak T., *J. Photochem. Photobiol. B*, **82**, 72—78 (2006).
48) Purcell M., Neault J. F., *Biochim. Biophys. Acta*, **1478**, 61—68 (2000).
49) Ferrer E. G., Bosch A., Yantorno O., Baran E. G., *Bioorgan. Med. Chem.*, **16**, 3878—3886 (2008).
50) Costa P., Sousa Lobo J. M., *Eur. J. Pharm. Sci.*, **13**, 123—133 (2001).